Understanding the final-state control from the standpoint of the model predictive control and its application to a three-dimensional trajectory control problem

Susumu Hara[1] · Ryuya Yokoo[1] · Kikuko Miyata[1]

Abstract
In many motion control problems of mechatronic equipment, the control performance of the final-state of the control period is strictly important for positioning or settling issues. Totani and Nishimura proposed a final-state control (FSC) method using the compensation input for achieving such requirements in 1994. The FSC technique has been improved and applied to various kinds of actual mechanical motion control problems. In the same way, there is a similar method to solve these kinds of problems called Model Predictive Control (MPC). However, the difference between FSC and MPC has not been fully clarified yet. This paper shows the relationship between the FSC and MPC methods. First, an updating-type FSC (UFSC) proposed by a part of the authors is introduced. Then, this paper analytically shows that the control input of UFSC agrees in the input of MPC under some conditions. This analysis makes clear the meaning of "updating" in the FSC technique for actual mechanical motion control applications. Moreover, this paper shows an application of the UFSC to a three-dimensional positioning problem with a fixed-wing airplane and performs numerical simulations to help the understanding the characteristics of the UFSC. Through the discussions of this paper, the characteristic of the FSC is clarified.

1 Introduction

In many motion control problems of mechatronic equipment, such information and precision equipment as hard disk drives and X-Y tables, the control performance of the final-state of the control period is strictly important for positioning or settling issues. Totani and Nishimura proposed a final-state control (FSC) method using the compensation input to solve these kinds of problems (Totani and Nishimura 1994). The FSC technique has been improved by some researchers and applied to various kinds of actual mechanical motion control problems (Hirata et al. 2005; Hirata and Ueno 2011, 2012; Ueda et al. 2017; Fujioka et al. 2014). In the same way, Model Predictive Control (MPC) has been widely applied to recent general control problems (Maciejowski 2002). The FSC technique looks similar to MPC, however, the relationship between FSC and MPC has not been fully clarified yet. Hara, *et al*. has presented the comparisons between the FSC technique and MPC methods (Hara et al. 2016; Miyata and Hara 2017; Hara et al. 2018). However, these papers focus on some special MPC methods (Kon et al. 2009; Ohtsuka 2004) and the comparisons are performed only with numerical simulations and real experiments. These discussions are not enough for understanding the differences between the UFSC and MPC methods. Therefore, this paper focuses on this topic.

The rest of the paper is organized in two parts. The first part deals with the mainly analytical comparison between the FSC and MPC. The second part shows numerical simulation examples.

The first part shows the relationship between the FSC and MPC methods from the viewpoint of the MPC in motion control problems, to help the understanding the FSC. First, an updating-type FSC (UFSC) proposed by Yoshiura and Hara. (Yoshiura and Hara 2014; Yoshiura et al. 2014). Then, this paper analytically shows that the control input of UFSC agrees in that of MPC under some conditions. This analysis produces another theoretical view of the FSC technique and makes clear the meaning of "updating" in the FSC technique for actual mechanical motion control applications.

The second part performs numerical simulations to help the understanding of the FSC. As mentioned before, the FSC methods are often applied to mechatronic equipment. Other applications have not been fully tried yet in contrast to many MPC applications. Therefore, this paper shows an application of the UFSC to a three-dimensional positioning trajectory generation problem with a fixed-wing airplane, performs numerical simulations, and

✉ Susumu Hara
haras@nuae.nagoya-u.ac.jp

Ryuya Yokoo
yoko.ryuya@h.mbox.nagoya-u.ac.jp

Kikuko Miyata
kmiyata@nuae.nagoya-u.ac.jp

[1] Department of Aerospace Engineering, Graduate School of Engineering, Nagoya University, Nagoya, Japan

helps the understanding of the FSC.

2 Final-State Control (FSC)

2.1 Original FSC (Totani and Nishimura, 1994)

FSC is a method for transferring the state of a dynamic system to a specified state in a specified time. The discrete-time state equation of the model of the n-dimensional dynamical system at the k-th sample is represented as follows:

$$\boldsymbol{x}[k+1] = \boldsymbol{A}\boldsymbol{x}[k] + \boldsymbol{B}\boldsymbol{u}[k], \tag{1}$$

where, $\boldsymbol{x} \in \mathbb{R}^n$ is state vector and $\boldsymbol{u} \in \mathbb{R}^m$ is control input vector. Here, only the controllable system is assumed. An input matrix $\boldsymbol{U} \in \mathbb{R}^{Nm\times 1}$ is considered under these constraints. The input matrix $\boldsymbol{U}$ transfers the state variables of the dynamical system from the initial state $\boldsymbol{x}[0]$ to the target state $\boldsymbol{x}[N]$ ($N \geq n$) and is expressed as:

$$\boldsymbol{U} = [\, \boldsymbol{u}^{\mathrm{T}}[N-1] \quad \ldots \quad \boldsymbol{u}^{\mathrm{T}}[1] \quad \boldsymbol{u}^{\mathrm{T}}[0] \,]^{\mathrm{T}}. \tag{2}$$

Generally, $\boldsymbol{U}$ is not determined uniquely. Therefore, a criterion function $\boldsymbol{J}$ is introduced to define the unique control input as follows:

$$\boldsymbol{J} = \boldsymbol{U}^{\mathrm{T}}\boldsymbol{Q}\boldsymbol{U}, \quad \boldsymbol{Q} > 0, \tag{3}$$

where, $\boldsymbol{Q} \in \mathbb{R}^{Nm\times Nm}$ is a block diagonal weighting matrix. The unique input $\boldsymbol{U}$ which minimizes Eq. (3) is:

$$\boldsymbol{U} = \boldsymbol{Q}^{-1}\boldsymbol{\Sigma}^{\mathrm{T}}(\boldsymbol{\Sigma}\boldsymbol{Q}^{-1}\boldsymbol{\Sigma}^{\mathrm{T}})^{-1}\{\boldsymbol{x}[N] - \boldsymbol{A}^N\boldsymbol{x}[0]\}, \tag{4}$$

where, $\boldsymbol{\Sigma} \in \mathbb{R}^{n\times Nm}$ is:

$$\boldsymbol{\Sigma} = [\boldsymbol{B} \quad \boldsymbol{AB} \quad \ldots \quad \boldsymbol{A}^{N-1}\boldsymbol{B}]. \tag{5}$$

In this way, FSC is known as a method of solving an optimal control problem with fixed-terminal-time and fixed-terminal-state, and has been widely applied to many mechanical motion control problems due to its useful characteristics.

2.2 Updating FSC (UFSC)

The original FSC is only valid for the problem whose final target is time-invariant. However, the target may be varied in real motion control problems due to the influences from the unexpected events such as disturbances, failures, and so on. Therefore, Updating FSC (UFSC) was proposed as an improvement of FSC (Yoshiura and Hara 2014; Yoshiura et al. 2014) in order to deal with the time-varying target state.

The scheme of UFSC is summarized in Fig. 1. In UFSC, the input matrix $\boldsymbol{U}$ is updated at certain intervals (*e.g.*, Figure 1 shows UFSC which updates input every sampling time.). Here, the input matrix of UFSC $\boldsymbol{U}_k \in \mathbb{R}^{(N-k)m\times 1}$ at k-th step is introduced as follows:

$$\boldsymbol{U}_k = [\, \boldsymbol{u}^{\mathrm{T}}[N-1] \quad \ldots \quad \boldsymbol{u}^{\mathrm{T}}[k+1] \quad \boldsymbol{u}^{\mathrm{T}}[k] \,]^{\mathrm{T}}. \tag{6}$$

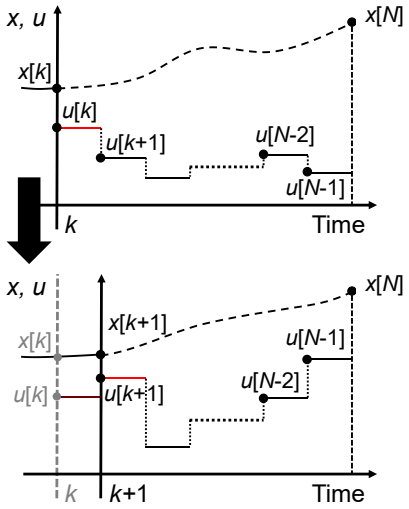

Fig. 1 Scheme of the updating final-state control (UFSC).

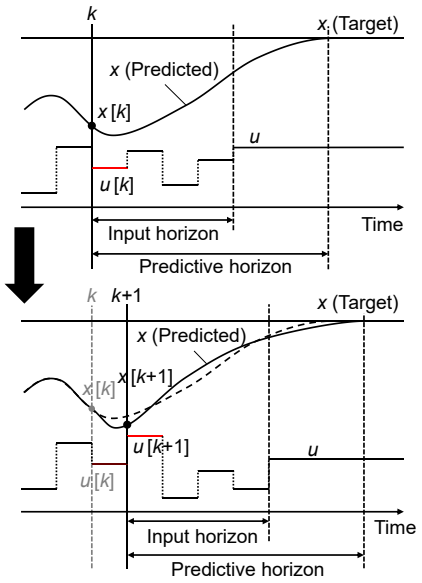

Fig. 2 Scheme of the model predictive control (MPC).

With an introduction to a block diagonal matrix $\boldsymbol{Q}_k \in \mathbb{R}^{(N-k)m\times(N-k)m}$ whose block diagonal entries are $m \times m$ positive definite matrices, Eqs. (4) and (5) are modified as:

$$\boldsymbol{U}_k = \boldsymbol{Q}_k^{-1}\boldsymbol{\Sigma}_k^{\mathrm{T}}(\boldsymbol{\Sigma}_k\boldsymbol{Q}_k^{-1}\boldsymbol{\Sigma}_k^{\mathrm{T}})^{-1}\boldsymbol{X}_k, \tag{7}$$

$$\boldsymbol{\Sigma}_k = [\boldsymbol{B} \quad \boldsymbol{AB} \quad \ldots \quad \boldsymbol{A}^{N-k-1}\boldsymbol{B}], \tag{8}$$

where, $\boldsymbol{X}_k$ is

$$\boldsymbol{X}_k = \boldsymbol{x}[N] - \boldsymbol{A}^{N-k}\boldsymbol{x}[k]. \tag{9}$$

Here, $N - k \geq n$ is required to obtain $(\boldsymbol{\Sigma}_k\boldsymbol{Q}_k^{-1}\boldsymbol{\Sigma}_k^{\mathrm{T}})^{-1}$ in Eq. (7). Therefore, $\boldsymbol{U}_k$ is not updated in $k < N - n$. Incidentally, the major part of the input matrix of UFSC is updated before it is used. Moreover, the input matrix does not have to be updated at every sampling step in UFSC.

Therefore, it is to be desired that only computes the part of the input matrix used for the inputs. With introducing updating interval l, Here, a modified input matrix $\boldsymbol{U'}_k$ can be which includes inputs from k-th step to $(k + l - 1)$-th step. Therefore, Eqs. (6) and (7) are modified as:

$$\boldsymbol{U'}_k = [\, \boldsymbol{u}^\top[k+l-1] \quad \dots \quad \boldsymbol{u}^\top[k+1] \quad \boldsymbol{u}^\top[k] \,]^\top, \tag{10}$$

$$\boldsymbol{U'}_k = \boldsymbol{Q}_{k,l}^{-1}\boldsymbol{\Sigma'}_k^\top(\boldsymbol{\Sigma}_k\boldsymbol{Q}_k^{-1}\boldsymbol{\Sigma}_k^\top)^{-1}\boldsymbol{X}_k, \tag{11}$$

where, for each $l \in \{1,2,\dots,N-k\}$, $\boldsymbol{Q}_{k,l} \in \mathbb{R}^{lm\times lm}$ is the lower right $lm \times lm$ block of the matrix $\boldsymbol{Q}_k$, and $\boldsymbol{\Sigma'}_k$ is:

$$\boldsymbol{\Sigma'}_k = [\boldsymbol{A}^{N-k-l}\boldsymbol{B} \quad \boldsymbol{A}^{N-k-(l-1)}\boldsymbol{B} \quad \dots \quad \boldsymbol{A}^{N-k-1}\boldsymbol{B}]. \tag{12}$$

In particular, in the case of UFSC updating inputs at every step (l = 1), input $\boldsymbol{U'}_k = \boldsymbol{u}[k]$ is obtained by the following equation:

$$\boldsymbol{u}[k] = \boldsymbol{Q}_{k,1}^{-1}\boldsymbol{B}^\top(\boldsymbol{A}^\top)^{N-k-1}(\boldsymbol{\Sigma}_k\boldsymbol{Q}_k^{-1}\boldsymbol{\Sigma}_k^\top)^{-1}\boldsymbol{X}_k. \tag{13}$$

3 Model Predictive Control (MPC)

3.1 MPC

Model Predictive Control (MPC) is an optimal-control method in a finite-horizon, and can consider control constraints. In general, horizons of MPC ("Input horizon" and "Predictive horizon" in Fig. 2) are receding every sampling step, and a certain optimal input is calculated simultaneously. The scheme of MPC is summarized in Fig. 2. Figures 1 and 2 suggest that the UFSC's scheme and MPC's scheme have similarities in both introducing predictive inputs. This similarity is obtained by introducing "updating" in the FSC technique.

In this paper, several constraints are introduced in MPC to clarify the relationship between MPC and UFSC analytically. At first, a predictive horizon is shrinking with its terminal fixed and input horizon is assumed to be the same as predictive horizon, to deal with fixed-final-time problem. Then, constraints such as inputs' limitations are not considered. Moreover, the stage costs are not included in the criterion function. Under these constraints, criterion function J_k at k-th step in MPC is expressed as:

$$J_k = (\boldsymbol{\Sigma}_k\boldsymbol{U}_k - \boldsymbol{X}_k)^\top\boldsymbol{P}_\mathrm{T}(\boldsymbol{\Sigma}_k\boldsymbol{U}_k - \boldsymbol{X}_k) + \boldsymbol{U}_k^\top\boldsymbol{Q}_k\boldsymbol{U}_k, \tag{14}$$

where, $\boldsymbol{P}_\mathrm{T} \in \mathbb{R}^{n\times n}$ is a positive definite matrix and $\boldsymbol{X}_k = \boldsymbol{x_T} - \boldsymbol{A}^N\boldsymbol{x}[k] = \boldsymbol{x}_k[N] - \boldsymbol{A}^{N-k}\boldsymbol{x}[k]$. The first term on the right-hand side is the terminal cost. It is incorporated instead of the terminal state constraint. The input matrix $\boldsymbol{U}_k$ minimizing Eq. (14) is obtained explicitly and rearranged as:

$$J_k = \boldsymbol{X}_k^\top\boldsymbol{P}_\mathrm{T}\boldsymbol{X}_k - 2\boldsymbol{X}_k^\top\boldsymbol{P}_\mathrm{T}\boldsymbol{\Sigma}_k\boldsymbol{U}_k + \boldsymbol{U}_k^\top(\boldsymbol{\Sigma}_k^\top\boldsymbol{P}_\mathrm{T}\boldsymbol{\Sigma}_k + \boldsymbol{Q}_k)\boldsymbol{U}_k. \tag{15}$$

Here, Eq. (15) is considered as a second-order convex function of $\boldsymbol{U}_k$. Generally, the following equation holds for general $\boldsymbol{Z}$ and $\boldsymbol{T}$, and general symmetric $\boldsymbol{S}$:

$$\boldsymbol{Z}^\top\boldsymbol{S}\boldsymbol{Z} + 2\boldsymbol{T}^\top\boldsymbol{Z} = (\boldsymbol{Z} + \boldsymbol{S}^{-1}\boldsymbol{T})^\top\boldsymbol{S}(\boldsymbol{Z} + \boldsymbol{S}^{-1}\boldsymbol{T}) - \boldsymbol{T}^\top\boldsymbol{S}^{-1}\boldsymbol{T}. \tag{16}$$

Equation (16) is completing the square for a quadratic multivariable function. Therefore, the $\boldsymbol{Z}$ minimizing Eq. (16) is clearly obtained as $\boldsymbol{Z} = -\boldsymbol{S}^{-1}\boldsymbol{T}$. By applying the method to Eq. (15), $\boldsymbol{U}_k$ minimizing J_k is obtained as follows:

$$\begin{aligned}\boldsymbol{U}_k &= (\boldsymbol{\Sigma}_k^\top\boldsymbol{P}_\mathrm{T}\boldsymbol{\Sigma}_k + \boldsymbol{Q}_k)^{-1}\boldsymbol{\Sigma}_k^\top\boldsymbol{P}_\mathrm{T}\boldsymbol{X}_k \\ &= \boldsymbol{Q}_k^{-1}\boldsymbol{\Sigma}_k^\top(\boldsymbol{P}_\mathrm{T}^{-1} + \boldsymbol{\Sigma}_k\boldsymbol{Q}_k^{-1}\boldsymbol{\Sigma}_k^\top)^{-1}\,\boldsymbol{X}_k.\end{aligned} \tag{17}$$

Here, the input used at k-th step is only the last block of $\boldsymbol{U}_k$. Therefore, the k-th input $\boldsymbol{u}[k]$ is expressed as:

$$\begin{aligned}\boldsymbol{u}[k] &= [\boldsymbol{0} \quad \dots \quad \boldsymbol{0} \quad \boldsymbol{I}]\boldsymbol{U}_k \\ &= \boldsymbol{Q}_{k,1}^{-1}\boldsymbol{B}^\top(\boldsymbol{A}^\top)^{N-k-1}(\boldsymbol{P}_\mathrm{T}^{-1} + \boldsymbol{\Sigma}_k\boldsymbol{Q}_k^{-1}\boldsymbol{\Sigma}_k^\top)^{-1}\,\boldsymbol{X}_k,\end{aligned} \tag{18}$$

where, $\boldsymbol{I} \in \mathbb{R}^{m\times m}$ is the identity matrix of order m.

3.2 Understanding the FSC technique from the standpoint of the MPC

Equation (14) includes the positive definite matrix $\boldsymbol{P}_\mathrm{T}$. $\boldsymbol{P}_\mathrm{T}$ means a weighting matrix of an error between the target state and a final state. Now, let us consider increasing $\boldsymbol{P}_\mathrm{T}$ for strictly conforming the final state to the target state. The increment of some elements in $\boldsymbol{P}_\mathrm{T}$ caused the increment of the matrix norm of $\boldsymbol{P}_\mathrm{T}$, and then the matrix norm of $\boldsymbol{P}_\mathrm{T}^{-1}$ decreases. This implies that $\boldsymbol{P}_\mathrm{T}^{-1}$ approaches a zero matrix. Therefore, when the error between the target state and the final state is reduced, Eq. (18) is expressed as follows:

$$\boldsymbol{u}[k] = \boldsymbol{Q}_{k,1}^{-1}\boldsymbol{B}^\top(\boldsymbol{A}^\top)^{N-k-1}(\boldsymbol{\Sigma}_k\boldsymbol{Q}_k^{-1}\boldsymbol{\Sigma}_k^\top)^{-1}\,\boldsymbol{X}_k. \tag{19}$$

Equation (19) clearly agrees with Eq. (13). It means that UFSC is a special form of MPC. In other words, the updating improvement of FSC technique in motion control applications corresponds to the addition of some model predictive function such as MPC. This result contributes to the augmentation of FSC ability to wider control problems.

In addition, some parameters can be compared to understand the relationship between these two methods. In this case, the N is the step to the final state in UFSC and the predictive step in MPC when the input horizon equals the predictive horizon. The UFSC originally focuses on the minimizing final state difference and the MPC also can focus on them taking large weight of the final state difference by using $\boldsymbol{P}_\mathrm{T}^{-1} \to 0$. The input is updated in every l sample step by UFSC and it becomes every step when we take l = 1. The MPC updates input every sampling period.

4 Simulation

4.1 Simulation model and conditions

As an example of the wider control problem applications, this section introduces numerical simulation examples of UFSC method applied to final state control problems. These examples show that UFSC method (or Eq. (13)) controls a system with given final states and fixed final time. As mentioned in Section 1, the FSC methods are often applied to mechatronic equipment and have not been fully applied yet to other problems, compared with wide MPC applications. Therefore, this section introduces a three-dimensional positioning trajectory generation of a fixed-wing airplane. The airplane trajectory is designed as satisfying the given target position and attitude (final states) at a given final time. The dynamics of the airplane is taken into account in order to keep the limitations of motion of the airplane.

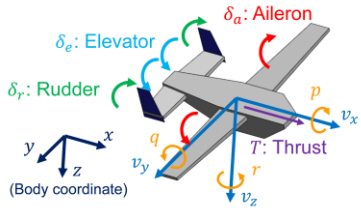

Fig. 3 A fixed-wing airplane model.

At first, a dynamical system of the fixed-wing airplane is expressed in Fig. 3. The system has 12-dimensional variable states $\boldsymbol{x}$ and 4-dimensional inputs $\boldsymbol{u}$ as follows (Roskam 1998):

$$\boldsymbol{x} = [v_x \ v_y \ v_z \ p \ q \ r \ \psi \ \theta \ \phi \ X \ \tilde{Y} \ \tilde{Z}]^\top, \tag{20}$$

$$\boldsymbol{u} = [\delta_a \ \delta_e \ \delta_r \ T]^\top, \tag{21}$$

where, v_x, v_y, and v_z are translation velocities, p, q, and r are angular velocities, ψ, θ, and ϕ are Euler angles, X, $\tilde{Y}$, and $\tilde{Z}$ are airplane displacements from a target position, δ_a, δ_e, and δ_r are steering angles of aileron, elevator and rudder respectively, and T is thrust of a propeller. Here, $\tilde{Y}$ and $\tilde{Z}$ mean reference displacements which enables the airplane entries the target point with entry horizontal angle Ψ_e and vertical angle Θ_e. Then, they are expressed as:

$$\tilde{Y} = Y\cos\Psi_e - X\sin\Psi_e, \tag{22}$$

$$\tilde{Z} = Z\cos\Theta_e - X\sin\Theta_e, \tag{23}$$

where, X, Y, and Z are airplane displacements on cartesian coordinate system fixed on the earth. The state equation including state variables (Eq. (20)) and inputs (Eq. (21)) is obtained by considering kinematics or dynamical forces affected on the airplane. The forces are derived from gravity, aerodynamics and control inputs. Here, the details of the dynamics or kinematics of the system are not concerned. The non-linear state equation is simply expressed as follows:

$$\dot{\boldsymbol{x}} = f(\boldsymbol{x}, \boldsymbol{u}). \tag{24}$$

Then, in order to handle the system with UFSC, Eq. (24) is linearized, discretized, and transformed into Eq. (1) form. Note that Eq. (24) is linearized and therefore $\boldsymbol{x}$ and $\boldsymbol{u}$ of Eq. (1) are replaced with displacement vector of state $\tilde{\boldsymbol{x}}$ and input $\tilde{\boldsymbol{u}}$ from equilibrium as follows:

$$\tilde{\boldsymbol{x}}[k+1] = \boldsymbol{A}\tilde{\boldsymbol{x}}[k] + \boldsymbol{B}\tilde{\boldsymbol{u}}[k], \tag{25}$$

where, $\tilde{\boldsymbol{x}} = \boldsymbol{x} - \boldsymbol{x}_{eq}$, $\tilde{\boldsymbol{u}} = \boldsymbol{u} - \boldsymbol{u}_{eq}$.

$\boldsymbol{x}_{eq}$ and $\boldsymbol{u}_{eq}$ are state variables and inputs at equilibrium. Finally, the system of Eq. (25) is handled with UFSC. Incidentally, Eq. (13) includes inverse matrix $(\boldsymbol{\Sigma}_k \boldsymbol{Q}_k^{-1} \boldsymbol{\Sigma}_k^\top)^{-1}$, so the regularity of it should be ensured. If $N-k$ is less than the dimension of the state variables $\boldsymbol{x}$ ($\dim \boldsymbol{x}$), the regularity is not ensured. Therefore, when $N-k < \dim \boldsymbol{x}$, $\boldsymbol{u}$ is not updated and $\boldsymbol{u}$ calculated at ($N-\dim \boldsymbol{x}$)-th step is used.

An RC airplane is supposed to the simulation. Its fuselage length is about 2.3 m (from nose to tail), wings span is 2.7 m, weight is 12.8 kg, and airspeed is more than

Table 1 Principal parameters of the simulation.

Simulation time step t_{step}	1 ms
Sampling time of control t_{samp}	0.1 s
Updating period of inputs t_{upd}	0.1 s
Simulation duration time t_{f}	20 s
Weighting matrix $\boldsymbol{Q}_{k,1}$	diag [1 10^5 1 1]
Limitations of control angle δ_i	$\lvert\delta_i\rvert \leq$ 0.35 rad
Limitation of thurst T	0 N $\leq T \leq$ 178 N
Entry velocity V_{e}	22.87 m/s
Horizontal entry angle Ψ_{e}	10 deg
Vertical entry angle Θ_{e}	4.00 deg
Forward target position X_{T}	450 m
Leftward target position Y_{T}	100 m
Target altitude Z_{T}	0 m

Table 2 Final states and differences from target state.

	Final States	Differences
ψ_{e} [deg]	10.00	± 0.00
θ_{e} [deg]	4.32	+ 0.32
V_{e} [m/s]	23.63	+ 0.76
X_{e} [m]	450.13	+ 0.13
Y_{e} [m]	100.02	+ 0.02
Z_{e} [m]	0.03	+ 0.03

20 m/s at level flight. At the beginning of simulations, the airplane is on level flight. The principal parameters of the simulation are summarized in Table 1. Important parameters of UFSC are updating rate and weighting matrix. Inputs of UFSC is updated every sampling time ($t_{upd} = t_{samp} = 0.1$ s), and the weighting matrix is designed to reduce aileron angle input. Inputs have limitations and they are saturated when they exceed the limitations. 7 parameters at the bottom of Table 1 are related to final-state. Final-state includes target attitude (decided by V_e, Ψ_e, Θ_e) and target position (decided by X_T, Y_T, Z_T).

4.2 Results and discussion

Table 2 shows the final states and difference between final states and target state calculated by numerical simulation. The relative errors of attitudes are less than 10% from the target state, and the differences of positions are about 0.1 meters at most. The airplane system, which is a complicated non-linear system, is controlled to target position with target attitude by UFSC. Updating of FSC contributes to these results since re-calculation of inputs compensate approximation errors derived from linearization and discretization. Figure 4 shows the simulated flight trajectory. The top-left side is the initial position and the bottom-right side is the final position. The airplane turns left toward to the target position just after leaving the initial position, then flies in the phugoid motion, and adjusts the attitude near the target position. Figure 5 shows the time series history of the inputs. The inputs and their variation are low while the airplane flies far from the final position. However, the thrust input becomes large and even saturated just before final position. It results from UFSC reducing the differences in short steps. This tendency is suppressed by enlarging the interval of inputs updating. The UFSC tends to generate the thrust input for the errors compensation between the target state and current state only by the several steps just before the final position. Therefore, the thrust input changes in the small steps dramatically at that timing. The thrust input variance of each sampling time of control can be suppressed when the interval of inputs updating is set to be longer with the same sampling time of control. As references, the simulation results using a longer updating period, $t_{upd} = 1.0$ s are shown in Fig. 6 and Table 3. In this case, the inputs in Fig. 6 become smooth trajectories in comparison with those in Fig. 5. The flight trajectory, in this case, is very similar to that in Fig. 4.

This solution is based on the UFSC method. In the case of MPC, the problem is usually solved by considering input constraint $|u_i| \le \bar{u}_i$ ($i = 1, 2, \dots, m$). In this case, the solution of Eq. (15) becomes different from the UFSC results and cannot be solved explicitly. Therefore, we solve the following convex optimization problem to gain the input:

minimize

$$J_k = \boldsymbol{X}_k^{\top}\boldsymbol{P}_T\boldsymbol{X}_k - 2\boldsymbol{X}_k^{\top}\boldsymbol{P}_T\boldsymbol{\Sigma}_k\boldsymbol{U}_k + \boldsymbol{U}_k^{\top}(\boldsymbol{\Sigma}_k^{\top}\boldsymbol{P}_T\boldsymbol{\Sigma}_k + \boldsymbol{Q}_k)\boldsymbol{U}_k$$

subject to

$$u_i{}^2[k+1] - \bar{u}_i{}^2 \le 0 \ (i = 1, 2, \dots, m;\ l = 0, 1, \dots, N-1), \tag{26}$$

where, the control angle limitations are defined as the same values of Table 1 and the thrust limitation is defined as the half value of the Table 1.

As references, the simulation results using the weighting matrix $\boldsymbol{P}_T = \mathrm{diag}[10^6\ 10^4\ 10^6\ 10^4\ 10^6\ 10^4\ 10^4\ 10^6\ 10^4\ 10^6\ 10^4\ 10^4]$ and $\boldsymbol{R} = \mathrm{diag}[1\ 10^5\ 1\ 1]$ are shown in Fig. 7 and Table 4. The control performance can be varied with the selection of the weighting matrices. In this case, the inputs in Fig. 7 is under the limitation and the thrust input becomes smooth trajectories in comparison with those in Fig. 5. The final states differences from target state are comparable with the Table 2.

Another important point is the calculation cost. These simulations are performed under the following condition: MATLAB® R2017a with CPU: Intel Core i7-6700, 3.40 GHz; OS: Windows 10 64 bit. In the case of the UFSC, one cycle of updating only takes about 5 ms, which far less than 0.1 s which is sampling time. It means that UFSC can be implemented online. On the other hand, the constrained MPC requires more than 12 sec with CVX solver (http://cvxr.com/cvx/) which is longer computation time comparing with sampling time.

Table 3 Final states and differences from target state with a longer updating period, $t_{upd} = 1.0$ s.

	Final States	Differences
ψ_e [deg]	10.00	± 0.00
θ_e [deg]	4.10	+ 0.10
V_e [m/s]	22.87	± 0.00
X_e [m]	450.02	+ 0.02
Y_e [m]	100.00	± 0.00
Z_e [m]	0.03	+ 0.03

Table 4 Final states and differences from target state with constrained MPC.

	Final States	Differences
ψ_e [deg]	9.99	− 0.01
θ_e [deg]	4.37	+ 0.37
V_e [m/s]	22.96	+ 0.09
X_e [m]	450.00	± 0.00
Y_e [m]	99.992	− 0.01
Z_e [m]	0.00	± 0.00

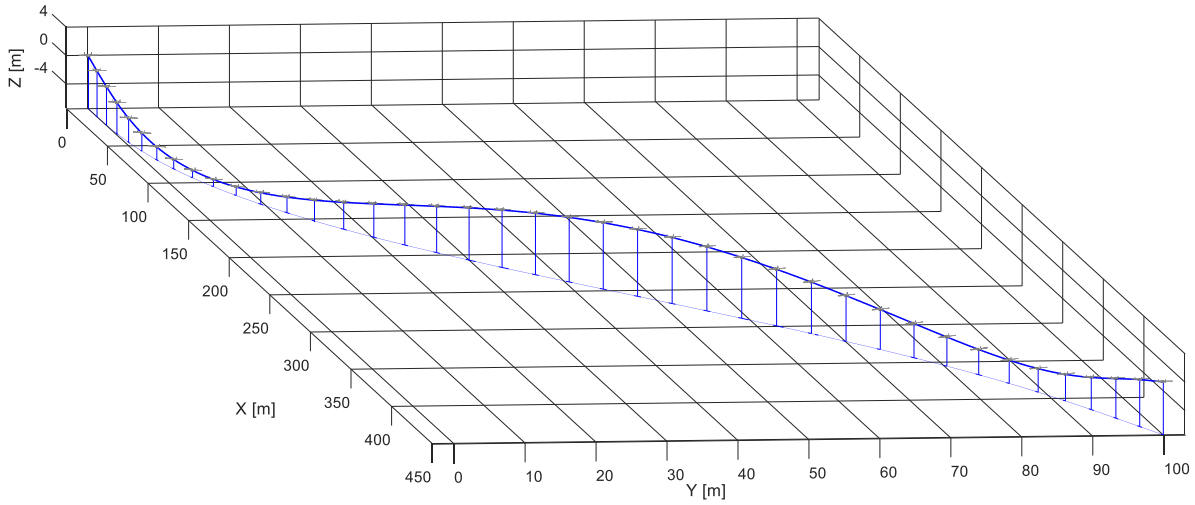

Fig. 4 Simulated flight trajectory. (Top-left is the initial position and bottom-right is the final position.)

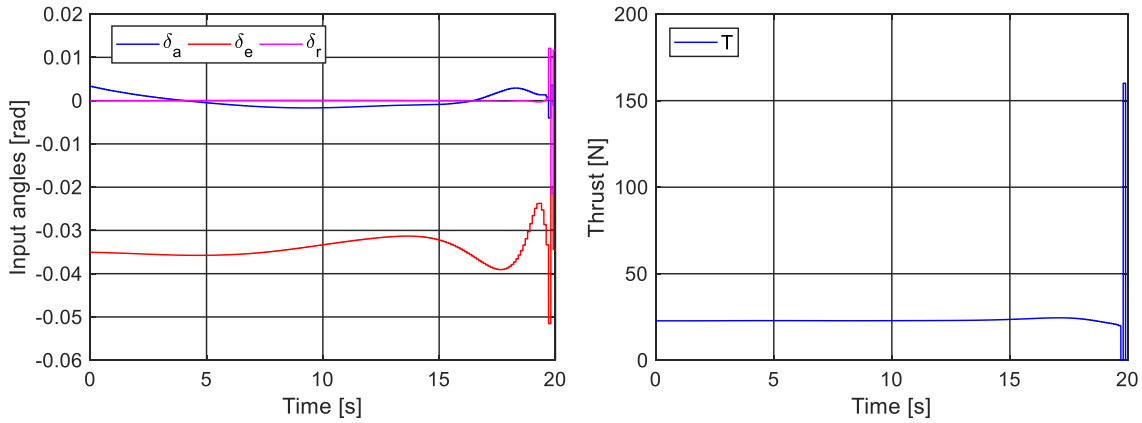

Fig. 5 Time series history of the control inputs. (Left: Control angles; Right: Thrust)

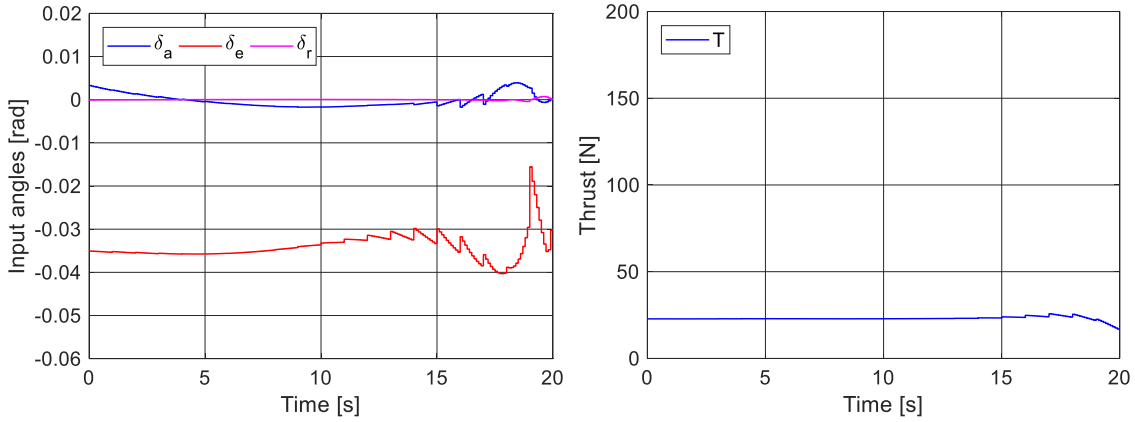

Fig. 6 Time series history of the control inputs with a longer updating preriod, t_{upd} = 1.0 s (Left: Control angles; Right: Thrust)

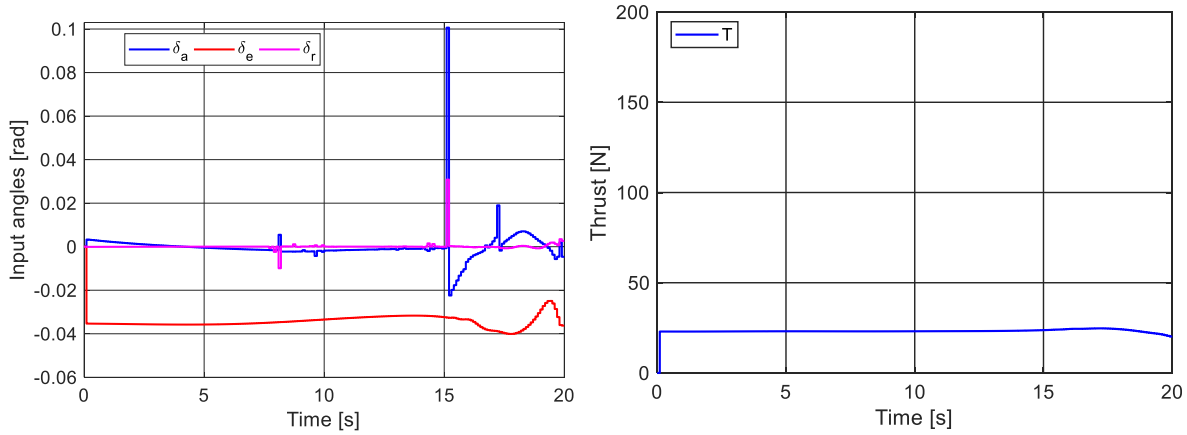

Fig. 7 Time series history of the control inputs with constrained MPC (Left: Control angles; Right: Thrust)

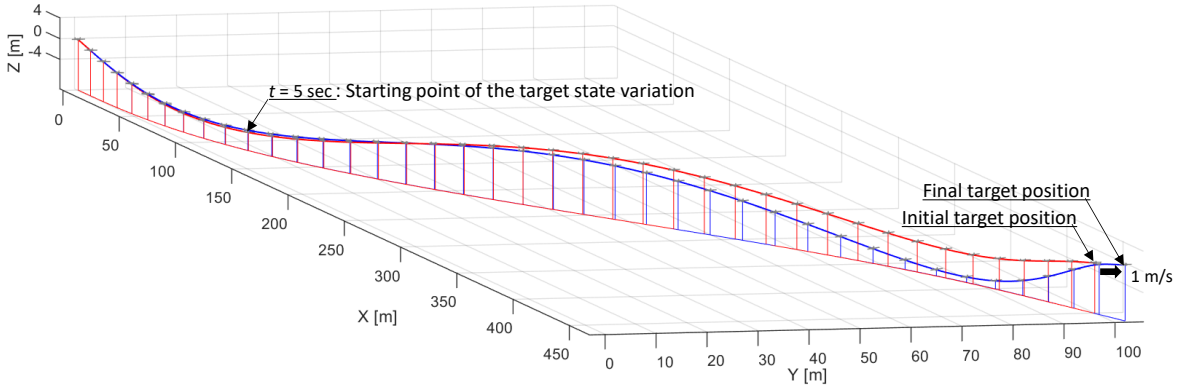

Fig. 8 Simulated flight trajectory. (Top-left is the initial position and bottom-right is the final position. Red: without final state variation, Blue: with final states variation)

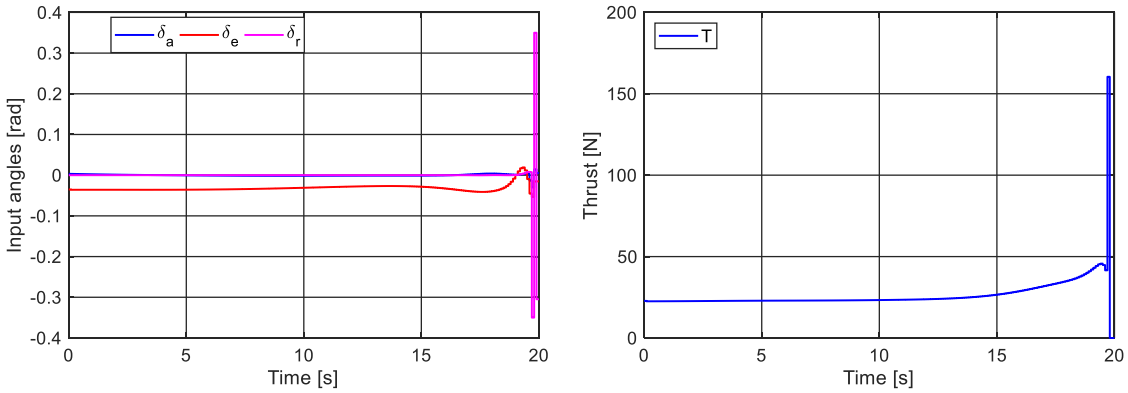

Fig. 9 Time series history of the control inputs with variable target state condition. (Left: Control angles; Right: Thrust)

4.3 Additional simulation

In addition to the previous section case, we set another numerical simulation condition which more focuses on the effect of the "updating" term in the UFSC. Here, we assume the same initial condition, control and simulation parameters explained in section 4.1. However, the target state variation occurs after 5.0 sec from the departure. This condition cannot be satisfied with the original FSC method.

The variation is set as the constant velocity Δv_x = 1.0 m/s. It can be assumed as the effect of the constant wind, for instance. The simulation results are summarized in Figs. 8 and 9. The red line in Fig. 8 is the original trajectory which is the exact same as Fig. 4. The blue line in Fig. 8 shows the final generated trajectory affected by the constant velocity. In the beginning, the trajectory is the exact same but the difference becomes larger because the

target state difference becomes larger. The final state results are summarized in Table 5. Here, the target position is varied because of the velocity effect. The errors become larger but it shows acceptable values in this numerical simulation. Figure 9 shows the time series history of the control inputs. The thrust tendency is almost the same as the Fig. 5 but the control angle variation becomes larger than Fig. 5. In addition to the thrust input variation, the rapid control angle variation is occurred to compensate the errors between the target state and current state only by the several steps just before the final position. The result shows the effectiveness of the "updating" the final states.

Table 5 Final states differences under the variable target state condition.

	Final States	Differences
ψ_e [deg]	9.56	− 0.44
θ_e [deg]	4.91	+ 0.92
V_e [m/s]	26.34	+ 3.47
X_e [m]	465.16	+ 0.16
Y_e [m]	102.64	− 0.03
Z_e [m]	1.08	− 0.02

5 Conclusion

This paper supports understanding the characteristic of the Final-State Control (FSC). First, the relationship between FSC and Model Predictive Control (MPC) methods were discussed analytically. The results showed that the control input in the Updating FSC (UFSC) in the previous study by a part of the authors could be obtained by the MPC under some conditions. This result indicated another theoretical view of the FSC technique and made clear the meaning of "updating" in the FSC technique for actual mechanical motion control applications. Moreover, this paper introduced a three-dimensional positioning trajectory generation of a fixed-wing airplane to show the wide application varieties of FSC. The airplane satisfied the given final states at the given final time in simulations and the effectiveness of the UFSC was verified. Through the discussions of this paper, the characteristic of the FSC was clarified.

ACKNOWLEDGMENT

The authors thank Dr. Daisuke Tsubakino from Nagoya University for his variable suggestions.

REFERENCES

Fujioka T, Okajima H, Matsunaga N (2014) A design method of robust control system for three-inertia benchmark problem using model error compensator and frequency shaped final-state control. Trans SICE 50:861-868 (in Japanese)

Hara S, Miyata K, Suzuki K, Tsukamoto M (2018) Effectiveness evaluation of updating final-state control for automated guided vehicles motion control with collision avoidance problems. IEEJ J Ind Appl 7:358-368

Hara S, Tsukamoto M, Maeda T (2016) Study on motion trajectory generation based on updating final-state control. Proc JSME Tokai Branch 65th Annu Meet:603, Toyota, Japan

Hirata M, Hasegawa T, Nonami K (2005) Short track-seeking control of hard disk drives by using final-state control. IEEJ Trans Ind Appl 125:524-529 (in Japanese)

Hirata M, Ueno F (2011) Final-state control using polynomial and time-series data. IEEE Trans Magn 47:1944-1950

Hirata M, Ueno F (2012) Final-state control using a time-symmetric polynomial input. IEEE Trans Control Syst Technol 20:395-401

Kon K, Fukushima H, Matsuno F (2009) Trajectory generation based on model predictive control with obstacle avoidance between prediction time steps. Trans SICE 45:406-413 (in Japanese)

Maciejowski J (2002) Predictive control: with constraints. Pearson Educ, Upper Saddle River, New Jersey

Miyata K, Hara S (2017) Comparison of self-moving cart motion control methods for collision avoidance problems. Proc SICE Annu Conf 2017:1429-1432, Kanazawa, Japan

Ohtsuka T (2004) A continuation/GMRES method for fast computation of nonlinear receding horizon control. Automatica 40:563-574

Roskam J (1998) Airplane flight dynamics and automatic flight controls, part I. DARcorporation, Lawrence, Kansas

Totani T, Nishimura H (1994) Final-state control using compensation input. Trans SICE 30:253-260

Ueda S, Kuroki Y, Hirata M, (2017) Trajectory design of galvano scanner considering voltage constraint of current amplifier. Electr Eng Jpn 198:54-64

Yoshiura T, Hara S (2014) Proposal of updating final-state control and its application to a connection control problem. Proc 13th Int Workshop Adv Motion Control:681-686, Yokohama, Japan

Yoshiura T, Hara S, Morita Y, Sato N, Yamada Y (2014) Manual motion control for connection and cooperation of plural mechanical systems. Proc 12th Int Conf Motion and Vib Control:2C13, Sapporo, Japan